ÉCOLE POLYTECHNIQUE
FÉDÉRALE DE LAUSANNE

Laboratory of Quantum Magnetism

Miniature Susceptometer Use in Pressure Cell

Physics Master - Travaux Pratiques TPIVb

Cevey Laurent

Under supervison of Julio A. Larrea Jiménez
and Henrik M. Ronnow

June 15, 2009

Contents

1 Introduction

This report presents the work done for my TPIV laboratory work, second semester of Master. It was carried out at Laboratory of Quantum Magnetism (LQM), at EPFL, under supervision of Pr. Henrik Ronnow. The work consisted in a research project, which was the continuation of the project carried out in the first semester, also at LQM.

Last semester's project allowed the construction, calibration, and first tests of an original miniature susceptometer (denoted MSM) for measuring AC magnetic susceptibility under high pressure. The first tests were performed in a temperature controlled environment (the SQUID apparatus in our laboratory), and occasionally in liquid Nitrogen and Helium. Those tests showed that the susceptometer's sensitivity would mainly make it useful for measuring relatively strong signals, like superconducting transitions. Thus, the initial goal of the project: measuring $SrCu_2(BO_3)_2$ (SCBO) [1] has then switched to measuring superconducting transitions, more precisely the evolution of T_c or other phase transition temperatures as a function of pressure in high temperature superconductors (HTS).

The subject of this project, susceptibility measurements under high pressures, present more difficulties and challenges when compared for example to transport measurements. As was

already presented in the article-type report of first semester, one has to cope with the fact that the high-pressure setup usually only allow measurement of very small samples, more specifically, small sample to detection apparatus size ratio. An advanced - but not standardized - method for measuring susceptibility would be to use a SQUID magnetometer (such as the "Quantum Design Magnetic Property Measurement System MPMS-XL1").
A challenging method to increase sensitivity of these susceptibility measurements without use of a SQUID device is to place the pick-up coils directly in the pressure medium. Having clamp-type pressure cells as the high pressure measurement method in our laboratory, the present project proposes to use a miniature susceptometer fitting inside the pressure cell. It can be noted that similar approaches have also been pursued in the case of sapphire anvil cells [3].

The work of this second semester will now be presented in a moreless chronological manner, describing the evolution, different steps and results of the project. Emphasis is put on the experimental work, in particular the preparation and use of a new clamp type pressure cell.

2 Iron pnictides litterature search and review

A most recent subject of interest is the new family of high temperature superconductors: the Iron Pnictides, which were first discovered in 2008. The pnictides first exhibited spontaneous superconducting behaviour for $T_c = 26$ K in electron-doped $La(O_{1-x}F_x)FeAs$, and later up to $T_c = 56$ K for $Sr_{0.5}Sm_{0.5}FeAsF$. High pressure studies are playing an important role in the process of understanding high temperature superconductivity (HTS) [2], they have a potential to underline instructive phenomena in the new members of extending pnictide family. Pressure indeed allows to explore a dimension of the compositional phase diagram, and can help distinguish the various effects of chemical doping (electron density, sutrctural distortions, local disorder, etc.) playing in the HTS properties.
In the perspective to perform a novel magnetic susceptibility temperature dependence measurement under high pressures, the recent litterature on high pressure studies was browsed through (based on the recent review by P.C.W. Chu [2] and references therein).

The result of this litterature search was that susceptibility measurements under pressure for electron-doped compounds of type $Ae(Fe_{1-x}Co_x)_2As_2$ (the 122 series), Ae = alkaline earth, such as $Ba(Fe_{1-x}Co_x)_2As_2$, $x = 0.08$, or $Ca(Fe_{1-x}Co_x)_2As_2$ are not very often presented. Moreover, looking for alternatives to FeAs-superconductors but with similar layered

structures, the compounds $FeSe_x$, $FeTe_x$ (the 011 series) are also of interest and generally appreciated because of absence of Arsenic. Studying this family's properties under pressure should be particularly interesting, as noted in [2]: "The simple structure and the unusually large positive pressure effect on Tc of the FeSe 011 phase may help unveil the mystery of superconductivity in Fe-pnicties and in cuprates in general." More recently, transport, susceptibility and x-ray diffraction measurements under high pressure showed structural phase transitions in $FeSe_x$ [6] and $FeTe_x$ [7].
Single crystal samples of $Ba(Fe_{1-x}Co_x)_2As_2$, $FeTe_x$ and $FeTeSe_x$ are presently available in the laboratory, allowing to perform various measurements once the pressure environment will be ready for implementing the MSM.

3 Susceptometer calibration: ambient pressure and pressure cell background tests

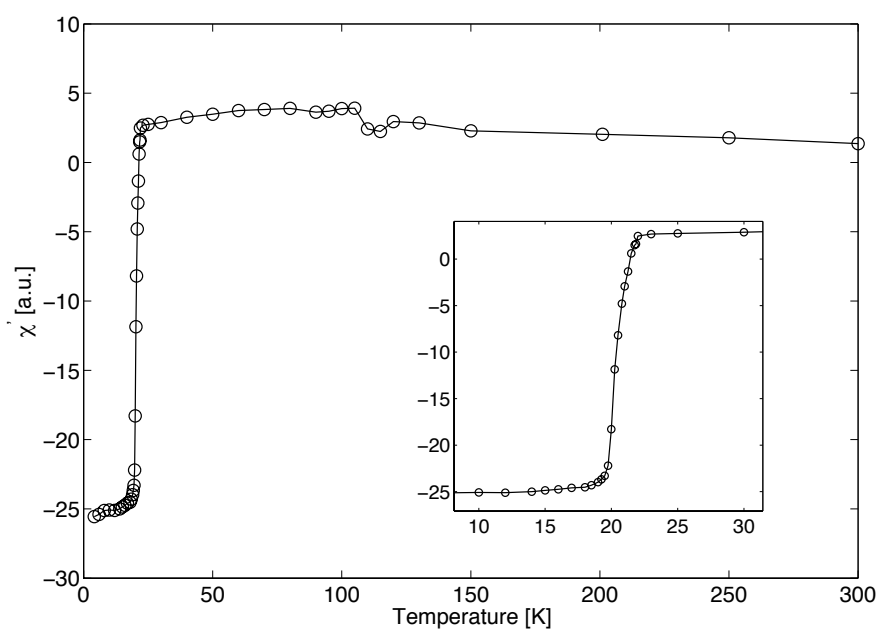

Figure 1: Real part of the //ab in-plane susceptibility of $Ba(Fe_{1-x}Co_x)_2As_2$, $x = 0.08$ obtained with the MSM in the SQUID temperature controlled environment. The inset shows a clearer view of the superconducting transition. The units are millivolts, as directly measured from the pick-up coils. An AC magnetic field of averaged strength 0.12mT is applied from running a 1mA current in the primary coil.

Most of the calibration work was completed by the end of last semester, but only few measurements examples were presented. As a control of the MSM capacity to measure HTS samples and sensitivity, a temperature scan was performed in the SQUID temperature controlled environment at ambient pressure, although this environment was previously shown to yield important stray signals. Temperature scan were performed manually, and the background was substracted based on previous measurements with empty coils.

Figure 1 presents the result for one of the compound of interest: $Ba(Fe_{1-x}Co_x)_2As_2$, $x = 0.08$, for a flat single crystal sample of size 2x0.9 mm and mass $m = 1.5$mg. A clear, quite abrupt transition is visible, which should be a good sign for further measurement of those compounds.

Another important calibration test was to see the change of signal in our susceptometer when inserted in the pressure cell. The design of our susceptometer and calibration work on the number of turns have allowed to cancel various background signals in vacuum and room temperature, but this cancellation is bound to change with temperature, even more with a magnetic or metallic environment. The background signal information might be critical as signal to noise ratio remains one of the difficult part to complete in this project. However, we won't aim at further improving the calibration (which could be done by adding compensation coils outside the cell as for example in [3]) but simply probe how large is the signal change between in and outside the pressure cell.
Measurements have been performed for background signal and a piece of iron wire (diameter $d = 0.8$mm, length $L = 2.5$mm), sticking the MSM in and outside of the pressure cell, at room temperature or in liquid nitrogen. An excitation current $A = 1$mA at frequency $\nu = 990$Hz was given by a current source. The results are summarized in the following table:

	Background signal [μV]	Iron wire [μV]
Room temperature outside cell	$U_{\Re} = 2.2$-3.5, $U_{\Im} = 0.06$	$U_{\Re} = 134.75$, $U_{\Im} = -0.4$
Liquid N_2 outside cell	-	$U_{\Re} = 135.8$, $U_{\Im} = -0.57$
Liquid N_2 outside cell (*)	$U_{\Re} = 6.46$, $U_{\Im} = -4.1$	-
Room temperature inside cell	$U_{\Re} = 12.51$, $U_{\Im} = -15.96$	-
Liquid N_2 inside cell	$U_{\Re} = 17.1$, $U_{\Im} = -18.42$	$U_{\Re} = 146.35$, $U_{\Im} = -16.74$

Where the line marked with (*) was obtained previously at liquid N_2 temperature ($T = 77$K) in the SQUID environment. These values show that a certain stray signal is induced by the presence of the cell surrounding the susceptometer, both in the real and imaginary parts of the susceptibility. It has to be noted that we use $U_{\Re}$ and $U_{\Im}$ to refer to the real and

imaginary part of *susceptibility*, which are respectively given by the imaginary and real part of *pickup signal* if defining the excitation current real. Indeed, the pickup inductance signal is shifted 90 degree from the excitation current.
We see that the real part of susceptibility is increased by the presence of metallic surroundings, while the imaginary part obtains a certain negative value. Meanwhile, lowering temperature from room to liquid nitrogen temperature leads to slight 1-4μV increase in the real part and 0-4μV more negative imaginary part. The signal inside the cell is relatively large when compared to the calibrated background value of the signal at room temperature, and coherent when compared to the previous signal obtained at liquid nitrogen temperature in the SQUID environment, in which metallic elements and even magnets were surrounding the susceptometer. In summary, background variations due to cell and cooling is on the order of 10-30μV ($\Delta|U| = \sqrt{17^2 + 18^2} = 25\mu$V), which is non-negliable compared to the 140μV signal from the iron sample, which has a relatively large susceptibility.

The increase of the real part of susceptibility can be understood in terms of induction in the following way. Induction works by definition against the change of magnetic flux. In the measured pickup signal $U_A - U_B$ where A (B) refers to the secondary on the inner (outer) part of the coil, the outer coil is closer to the wall and thus feels a stronger magnetic field from induced currents in the walls, that we call induced field. For our measured signals U_A and U_B, most of the competition between applied field and induced field happens inside the primary coil, where the induced field has a negative amplitude compared to the field from the primary coil thus fields tend to cancel each other (a constructive part between the fields exists outside the primary coil, among the turns of secondary B which can be felt by the external turns, but it should have a minor influence). Thus both signals from the pickup coils are reduced in amplitude, but U_B is more reduced than U_A as it receives a larger part of the induced field flux both in field amplitude and area. Finally, this results in an increase of the real part of the pickup signal.

These measurements however only account for two specific temperatures. A measure of the cell background signal as a function of temperature is still to be performed once the susceptometer will be set in the pressure cell. A background substraction might be necessary, but this brings up the difficulty of reproducing very similar conditions (in pressure, external magnetic field) of an experiment. We also saw that background signal doesn't simply add up with and without sample, which suggests a certain $\approx 5\mu$V uncertainty, and

irreproducibility of the background for different samples. Eventually the effect of pressure on the susceptometer itself (geometry and components properties) might bring up more complications.

4 Pressure cell work

Getting nearer to the application of the MSM in the final pressure cell environment, preparation and testings of the pressure cell were done. The cell is a clamp type pressure cell, made of beryllium-copper, which is a material of choice having a high strength over large range of temperatures, and a good thermal conductivity.

4.1 Preparation of the new pressure cell

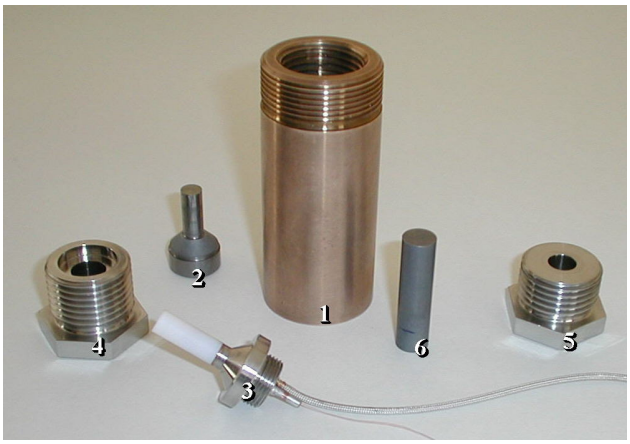

Figure 2: Advertising picture of main components of the CC33 nonmagnetic optical pressure cell (source: [5]) which we reproduced. 1 - Body, 2 - Piston, 3 - Obturator, 4 - Screw for piston, 5 - Screw for obturator, 6 - Push rod.

A new pressure cell was built by the IPMC (Institut de Physique de la Matière Condensée) workshop of EPFL, based on an AutoCAD design of the commercial Russian CC33 nonmagnetic pressure cell [5], the latter might achieve pressure up to 28 kbar. Figure 2 shows a representation of the commercial cell in a slightly different model. $BeCu$ material was used to fabricate the main components of the new pressure cell including the inner cylinder which is a key component to achieve the limit of high pressures. In case of the commercial Russian cell, the outer cylinder is made of $BeCu$, while the inner cylinder is made of a Ni-Cr-Al alloy. It should be noted that this alloy is not a commercial material, thus $BeCu$ may be

an alternative material to fabricate the inner cylinder as well. Nevertheless, $BeCu$ is a mechanically softer material than the Ni-Cr-Al alloy, thus we expect a lower achievable limit of pressure for our cell in comparison with the Russian CC33 pressure cell. This difference in composition of our cell is thus a very relevant information to find out the limit of high pressures that our "home made cell" can achieve.
We can note that the outer-inner cylinder design allows the method of *autofrettage*. This method consists in using a slightly larger insert than the inner size of the outer cylinder, which requires some method for fitting it in, and results in a spontaneous strain from the outer cylinder on the insert, increasing the maximum pressure. Various preparation work was needed, before testing the pressure performance of this new cell.

A heat treatment was applied to the body and two end screws (the lower and upper locknuts) of the cell, and optimally set at a temperature 315 C for 3 hours. The heat treament was made in the air, with a certain temperature ramp ($\approx$ 20min) before and after the treatment to avoid brutal change of temperature. The hardness was measured using an indenter tool, with the following results before and after the treatment:

Material type	Vickers Hardness	Pressure [kbar]	Max P tolerance [kbar]
BeCu before treatment	241	23.63	8
BeCu after treatment	375-420	36.78-41.19	13-15

Where the conversion between Vickers Hardness and pressure is given by 1 [HV]$\rightarrow$ 0.09807 [kbar]. However these values cannot be taken directly as the highest pressure that $BeCu$ could tolerate, these values have to be interpreted using one's own experience. Richard Gaal made the interpretation and could estimated the corresponding maximum pressure tolerance of about 15kbar for the $BeCu$ body of the pressure cell. This corresponds to the known limit of $BeCu$, where one also has to consider the other parameters of the experiment, namely the temperature cycles that will be done, giving a certain strain on the material. Thus our cell is optimally prepared for applying pressure and we will apply pressure up to about 15kbar, where the actual pressure has to be determined using different probes as discussed further.

4.2 Obturator and feedthrough preparation

In the process of preparing a pressurization with our cell, a critical step is the preparation of the obturator and the wires feedthrough. As the obturator is the supporting piece on which will sit the pressure medium in the teflon cap, the feedthrough need to be most carefully

prepared with *stycast* epoxy (Stycast 2850 FT) to avoid a leak of the pressure medium.

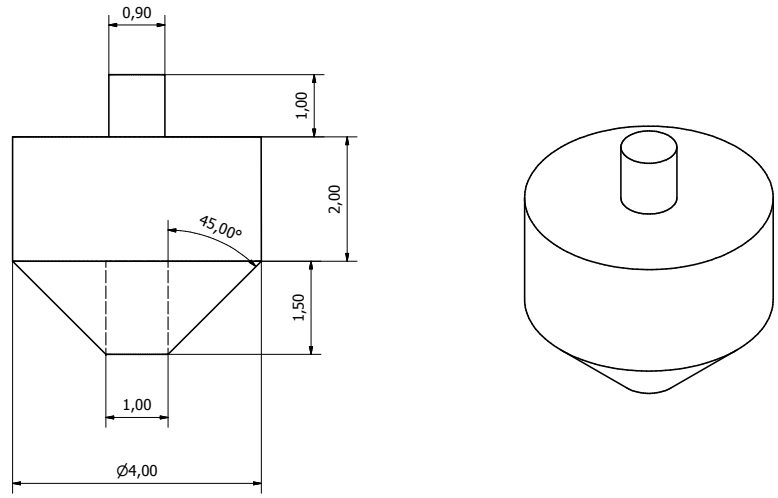

Figure 3: Scheme of the mounting piece for the MSM to use for a new obturator.

A braid of 16 twisted wires was prepared, where special attention has to be payed in having clean wires. One needs to wear gloves to avoid putting grease and other dirt on the wires. Insulation is scratched off with a knife at one end of the feedthrough wires, for further silver paint connections on the obturator side. Solders contain superconducting compounds and could thus give large perturbations in the susceptibility measurements, thus soldering should be avoided in the pressure medium. The obturator was then set on a tube linked to a pump, and after careful setting of the wires in the barrel, stycast was applied in the upper hole and warmed up to improve fluidity, and pumped through the barrel by vacuum.
The first obturator prepared for the purpose of testing the pressure cell has a carbon fiber rod intended for holding the coil, but a new obturator with a better mounting piece - see figure 3 - is foreseen.

4.3 Applying and probing pressure

Pressure was applied using a hydraulic press. The press displays a value of applied pressure (load) $P_{\text{hydraulic}}$ ranging from 0 to 40 MPa, which has a certain correspondence to the actual pressure P reached inside the pressure cell. The conversion is characteristic of the press, and is a priori given by a calibration curve. However for the new pressure cell, the pressure has to be probed to check this calibration, as slight differences (e.g. from friction) might occur.

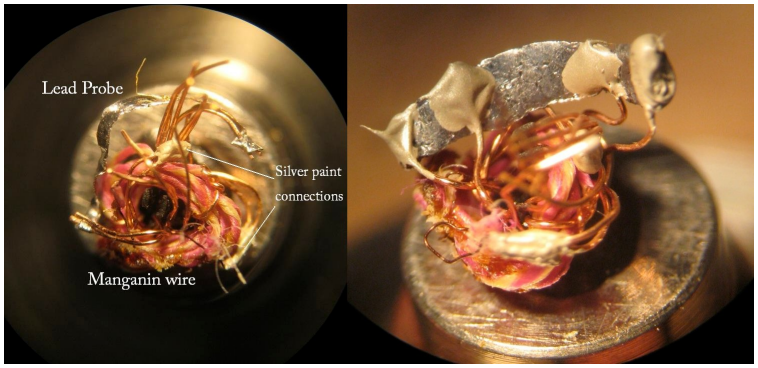

Figure 4: Microscope top-view of the mounted obturator with the two probes visible. The right hand side shows a different lead probe with clear 4-points probe.

Among the tools for probing the pressure, two are used with best application for certain range of pressure. A 4-point resistance measurement on a *Manganin*-gauge is good for pressures up to a few kbar, and measuring the variation of Lead superconducting transition temperature T_c also works towards higher pressures (up to 150kbar).
Fig. 4 is a microscope top-view of the obturator with the 2 probes set.

4.3.1 Room temperature measurements

As we apply pressure to the cell at room temperature, the resistance values of the Manganin gauge and the lead can be measured as a function of pressure. Figure 5a presents the pressure dependence of Manganin for two different runs. The second run presented some peculiar effects when starting to apply the pressure. A maximal pressure of 12 MPa was applied from the press, the corresponding pressure of which still needs to be determined. Manganin can hereby give an evaluation of the obtained pressure as a function of resistance change through the formula:

$$P\ [\text{kbar}] = a\Big(\frac{R(P)-R_0}{R_0}\Big) + b\Big(\frac{R(P)-R_0}{R_0}\Big)^2 \tag{1}$$

with $a = 395.3$, $b = 200$ and R_0 is the resistance at $T = 20$ C and $P = 1$ atm. This formula seems good to use on the first run, taking R_0 as the first measured value for $P_{\text{hydraulic}} = 0$, where the nearly constant values for low applied pressure can be understood from different points of view. First, friction effects, reduction of bubbles and other stabilization phenomena could make that pressure and thus manganin resistance doesn't increase so much when starting to apply pressure. Second and more probably, when the cell is set in the press, the

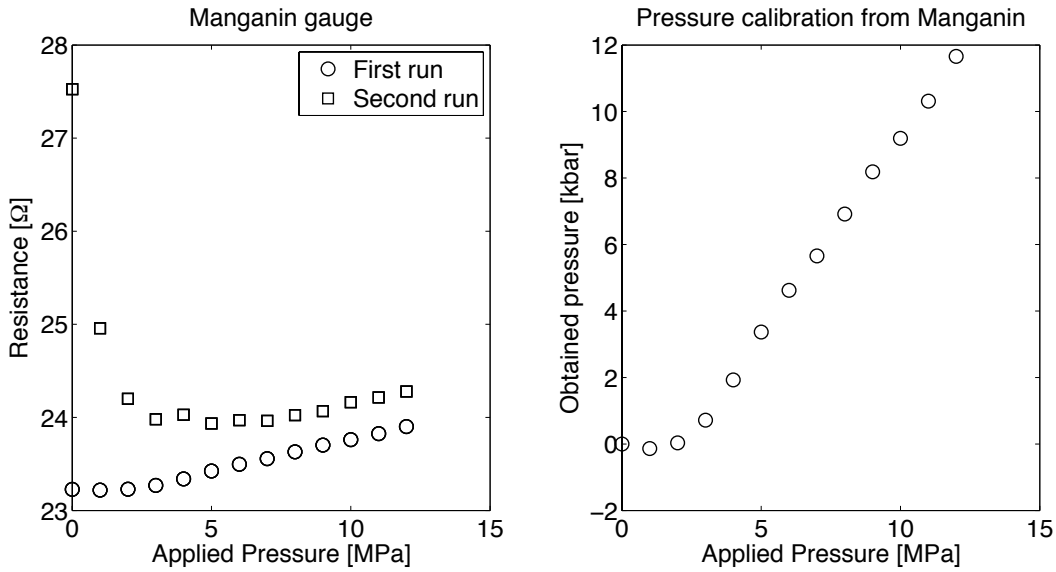

Figure 5: Room temperature resistance measurements of Manganin in two different runs. The right hand side shows a pressure calibration from the first run, using equation (1).

$BeCu$ upper locknut has already been tightened quite hard after pushing on the pressure medium cap with a cylinder, thus a certain pressure might already exist before applying a load. This would make us underestime the value of pressure as we take a probably too large R_0. However it is not easy to infer what should be the correct dependence, as equation (1) is not linear and we are not certain that the relation applied load to obtained pressure should be linear either. Nevertheless the result from using equation (1) with R_0 as the first value is shown on figure 5b. We see that the maximum pressure obtained is about :

$$P_{\max} \cong 12 \text{ kbar}$$

which might be an underestimation as was said before.

More tests and probing of pressure were done using the lead probe. The change of lead resistance as a function of pressure has been studied in a referenced article [4]. In that reference, a calibration based on well known structural phase transition points of Bi and Tl was made, in remarkably good agreement with measurements. Figure 6 proposes a fit of their reference curve to our measured curve. If we assume a simple proportional relation between applied and obtained pressure (as was approximately seen on figure 5b and can also be seen in the calibration curves for the Russian pressure cells), finding the proportionality factor between the reference curve and the experimental curve should give us another evaluation of

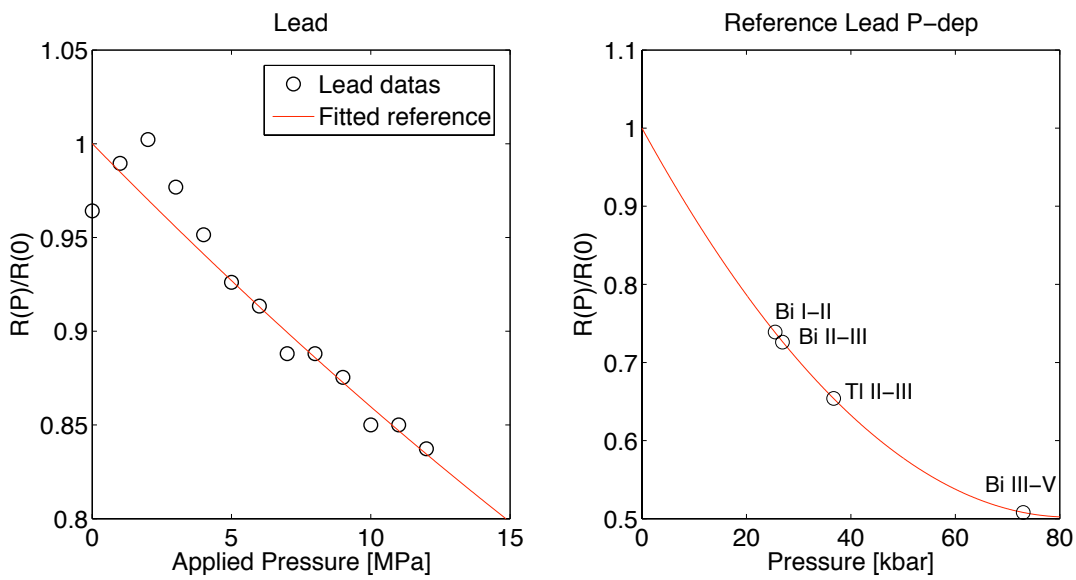

Figure 6: Attempt to fit our data of lead resistance pressure dependence on the left-hand side with the reference curve (from [4]) on the right-hand side, through a proportionality factor. The vertical axis is the ratio of resistance at pressure P with zero pressure resistance. The values of lead resistance run approximately from 60 to 85 mΩ on the graph.

the link between the applied load and the obtained pressure in the cell. However, this fitting parameter is hard to choose, as our data do not perfectly correspond to the shape of the reference curve. The optimal fit that we chose "by hand" in figure 6a and our assumption of a linear dependence brought the following relation :

$$P \cong 1.25 \left[\frac{\text{kbar}}{\text{MPa}}\right] \cdot P_{\text{hydraulic}} \quad \Rightarrow \quad P_{\text{max}} \cong 15 \text{ kbar}$$

Again this value suffers an approximative fit, in particular the zero pressure resistance $R(0)$ (to choose the reference fit y-intercept) had to be approximately evaluated, as a peculiar behaviour is observed for low applied pressure : we expect a monotically decreasing curve as in the reference curve instead of the bump that we obtained. It should be noted that the curve generally presents much scatter, from which could just originate the difference on the 2-3 first data points. High stability and precision are hard to achieve for such low signals of milli-Ohms.

This tells us that another step is necessary to determine the pressure achieved in the cell.

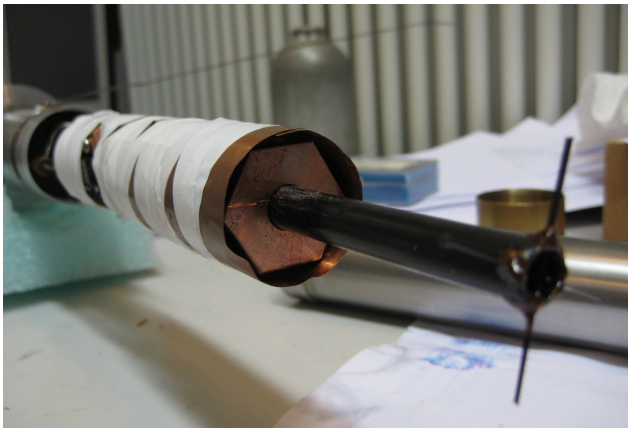

Figure 7: Picture of VTI set up. A copper foil was used to folder the cell in the second stage of measurements to improve thermalization. The plastic stick with "star end" helps to avoid the cell touching the chamber walls.

4.3.2 Temperature dependant measurements

Once the cell is closed and pressurized, one way to probe the unknown pressure is to observe the shift of the lead superconducting transition. A variable temperature insert (VTI) is used as a temperature control. Figure 7 shows the set up for this measurement, where the stick is dipped in a Helium dewar for the measurement. A vacuum insulation between the inner chamber and the surrounding Helium is used to control the cooling rate, where a capillary with tunable opening lets Helium slowly flow from the dewar into a cooling chamber, which is then thermally connected to the pressure cell. This thermal contact is actually a critical point for our experiment. Indeed, for these temperature dependant measurements, the accurate value of the temperature at which the phenomena are observed is most important to determine. Thermalization of the set-up is then a critical parameter to control, which presents a major difficulty. The first thing it implies is that each of these measurements should be done with conditions as similar as possible, conditions such as the cooling rate, the wires and connections set-up which have to be carefully arranged not to have any contact with the surrounding walls. First, as a simplest setting, the temperature scan will be performed with the "natural" cooling rate of the VTI in the Dewar, which can be roughly controlled by the opening of the Helium pumping capillary, and by the height of the VTI in the Dewar. Lowering the VTI stick into the Dewar increases the rate of cooling.

As a certain thermal gradient cannot be avoided between the outside of the pressure cell and the pressure medium inside where the sample will sit, we first want to evaluate this

difference, which once known should be carefully reproduced for every measurement. This gradient ΔT_c can be measured using two lead probes, one sticking on the outer wall of the cell and the other inside as was seen on Fig. 4. A thermometer also sits outside the cell, thus we expect to observe the transition of the outer lead probe at a displayed temperature of about $T_c = 7.12$ K for the superconducting transition temperature of the pure lead probe that we are using. However the lead inside is separated from the outside - and from the thermometer - by the wall of the pressure cell, thus we expect to observe the superconducting transition at a different displayed temperature. The difference between those two observed transitions should thus give us the temperature gradient between the inside and the outside of the cell. Similarly, this can be used to measure the superconducting transition temperature shift due to pressure, which follows a linear curve.

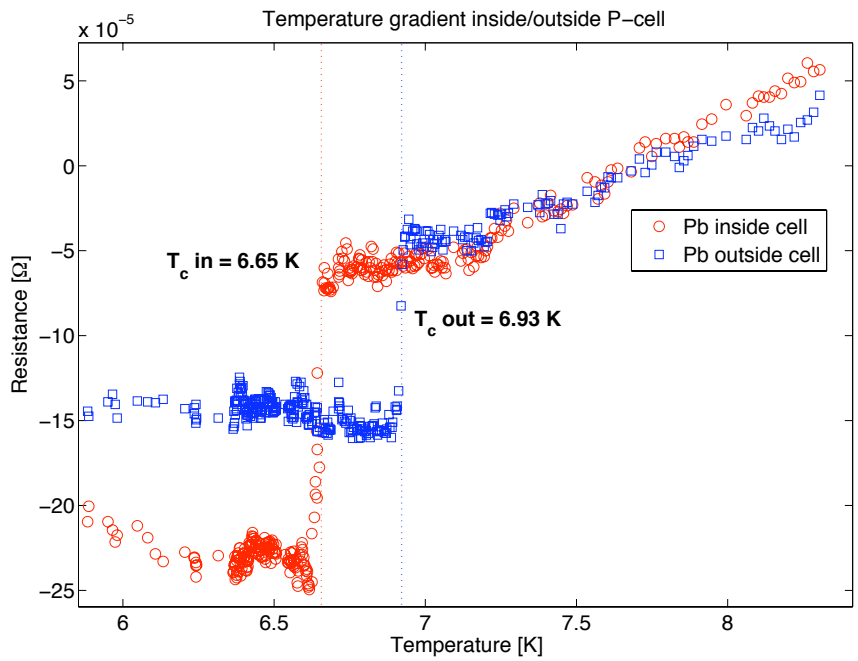

Figure 8: Observation of the temperature gradient between the inner and outer parts of the pressure cell. The data were obtained with a VTI, and taken cooling the cell. The negative values of resistance are due to the fixed offset of the measurement device.

The next step consisted in repeating this measurement after applying a certain pressure to the cell. The two lead probes are used again, and by measuring the new difference $\Delta T_c'$ between the SC transition temperatures and using the previous result at zero pressure, the

temperature shift of T_c due to pressure only should be expressed as :

$$\Delta T_P = \Delta T_c' - \Delta T_c$$

However, this expression will only be fully applicable under the condition that the temperature gradient keeps the same value ΔT_c in the second measurement. This condition can be assumed to be well respected if the transition temperature of the probe outside is the same than in the first measurement. Then the thermalization conditions should be similar as well as the cooling rate and thus ΔT_c.

The change of superconducting temperatures T_c of Pb as a function of pressure has been derived both on experimental and theoretical ground [4] and is given by the equation :

$$P = \frac{T_c(0) - T_c(P)}{0.365 \pm 0.003} \quad [\text{GPa}] \tag{2}$$

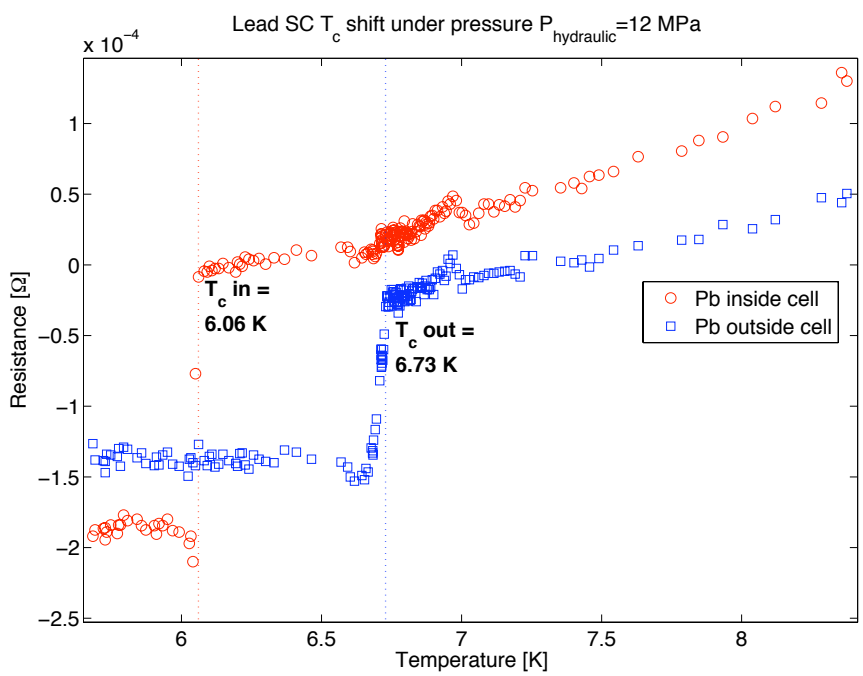

Figure 9: VTI measurement of the lead transitions shift under pressure with a load $P_{\text{hydraulic}} = 12$MPa. A larger difference is observed for the lead probes' T_c inside/outside, as expected with pressure.

Figure 8 shows the superconducting transitions of the two lead probes, inside and outside the pressure cell. In that first measurement, a temperature gradient $\Delta T = 0.28$ K was

observed. The measurement was repeated with the pressurized cell at a load $P_{\text{hydraulic}} = 12$ MPa, as shown on figure 9. However, we see that the transition temperature of the lead probe outside the cell is now quite different from the previous value at ambient pressure: $T_c$out $= 6.73$K versus $T_{c\ \text{out}} = 6.93$K. Thus this measurement cannot be safely used for determining an accurate value for the pressure, and it has to be repeated with a better conservation of thermal conditions, mostly the thermalization has to be improved.

4.3.3 Programmable temperature scans

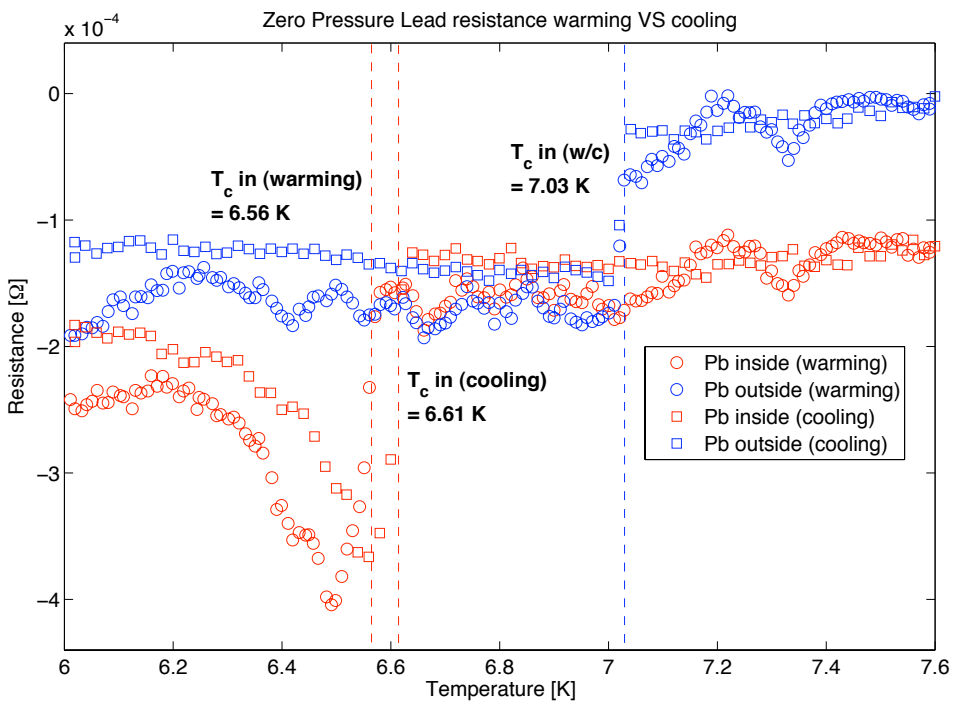

Figure 10: Comparison in the lead transitions between warming and cooling process, using the VTI and heater. Data were first gathered warming from the lowest temperature, and then directly cooling down. The cooling rate used is twice the warming rate, giving less points for the cooling curves.

A tool that can help us reproduce similar thermal conditions (cooling rate) already exists in the VTI. A heater attached to the cooling chamber allows to better control the temperature. A script then allows to perform temperature scan with given temperature boundaries and cooling/warming rate. Figure 10 shows such a measurement using a programmed tem-

perature scan, and compares the warming/cooling processes. As the scan was first taken upwards in temperature, we still observe a "faster" transition of the lead probe inside the cell, which suggests that the heater warms up the inside of the cell quicker than the outside. This difference is measured as $\Delta T = 0.46$ K. The cooling plot shows almost the same transition temperatures with a slight difference for lead inside: the transition is at $T_c = 6.61$ K instead of $T_c = 6.56$ K for warming, which corresponds to a lower gradient of $\Delta T' = 0.41$ K. This similarity shows that cooling occurs faster on the outside, but with a slightly better thermalization than the warming process as the gradient is now reduced. However these gradients are quite large, even larger than in our first plot 8 letting the system cool down without a temperature control. This shows that the thermalization conditions yet have to be improved, and the programmed temperature scan didn't help improve these. This could be improved by reducing the cooling/warming rate, and meanwhile, this still allows a good reproducibility of the conditions, which is necessary for extracting the T_c shift due to pressure.

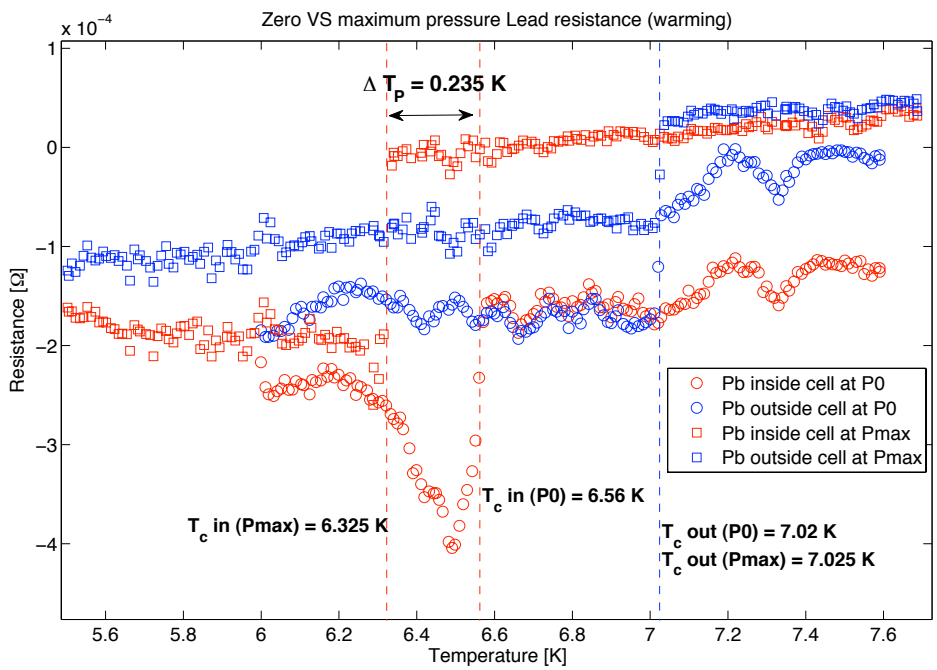

Figure 11: Comparison between the lead transitions inside/outside at zero pressure and applied pressure $P_{\text{hydraulic}} = 12$MPa. The data were obtained with the VTI with a programmed temperature scan.

Figure 11 displays two temperature scans in the warming direction, comparing zero pres-

sure and the maximum pressure of $P_{\text{hydraulic}} = 12$ MPa. The transition temperature for the lead outside is the same for both pressures, which shows the similarity of the thermal conditions, and lets us assume good enough conditions for extracting the transition temperature shift due to pressure only, and extrapolate the corresponding pressure using equation (2) :

$$\Delta T_P = 0.235 \text{ K} \quad \Rightarrow \quad P_{\text{max}} = 6.44 \text{ kbar}$$

This value is quite lower than we obtained with the pressure-dependence of lead and manganin's resistance (P_{max} = 12-15 kbar), thus we might again question the validity of this result. It should be noted that the lead probe has been replaced after breaking between the zero pressure and maximum pressure measurement, but the lead used being the same, it shouldn't give a difference in the observed T_c. This discrepancy with our previous results didn't bring full satisfaction in the original objective of accurately determinating the maximal pressure achieved by our cell. Anyhow, the thermalization should still be improved for the sake of our future measurements with the MSM.

5 Upcoming use of susceptometer in the pressure cell

Final implementation of the MSM in the pressure cell has not been completed by the end of the semester. The plan for continuing the project includes setting of the MSM in the currently used obturator. However, a neater set up could be done with a new obturator, using a supporting piece prepared by the workshop as seen on figure 3.

Regarding the issues of thermalization discussed in the last section, we will fabricate a new Cu cylinder to attach to the outer $BeCu$ cylinder of the pressure cell, which should work as thermal anchoring and help avoid critical thermal gradients between the inner (where the sample is fitted) and the outer (where the thermometer is attached) parts of the pressure cell.

Calibration measurements of signal temperature dependence with empty coils should be first carried out after setting the MSM inside the pressure cell, again with null and maximum pressure. However, it might be more fruitful and efficient to measure a sample as soon as possible, as the type of observation we want to make (a shift of T_c with pressure?) should not be much affected by background signals. Nevertheless, a good part of the work presented in this report was for the purpose of calibrating and accurately determinating the pressure in the cell, which is a more important piece of information.

As discussed in section 2, once the new obturator is completed and the MSM is ready for

measuring in the pressure cell, there will be several candidates as the sample crystals to measure, such as $Ba(Fe_{1-x}Co_x)_2As_2$, $FeTe_x$ and $FeTeSe_x$.

References

[1] L. Cevey, "Miniature AC susceptometer" (2009).

[2] C. W. Chu and B. Lorenz, Physica C 469, 385C (2009).

[3] P. L. Alireza and S. Julian, Rev.Sci. Instrum. 74, 4728 (2003).

[4] A. Eiling and J.S. Schilling, J. Phys. F : Metal Phys., 11 (1981).

[5] Institute for High Pressure Physics, Russian Academy of Science, "http://www.hppi.troitsk.ru/products/cc33_cell.htm", last viewed 09.06.09.

[6] V. G. Tissen et al, arXiv:0905.3289v2 (May 2009).

[7] C. Zhang et al., arXiv:0905.3249v1 (May 2009).